Digest Journal of Nanomaterials and Biostructures Vol. 6, No 2, April - June 2011, p. 779 - 790

BIOACTIVITY AND ANTIMICROBIAL PROPERTIES OF PMMA/Ag_2O ACRYLIC BONE CEMENT COLLAGEN COATED

S. CAVALU*, V. SIMON[a], G. GOLLER[b], I. AKIN[b]
University of Oradea, Faculty of Medicine and Pharmacy, 410068 Oradea, Romania,
[a]*Babes-Bolyai University, Faculty of Physics & Institute of Interdisciplinary Research in Bio-Nano-Sciences, 400084 Cluj-Napoca, Romania*
[b]*Istanbul Technical University, Metalurgical and Materials Engineering Dept, 34469 Maslak Istanbul, Turkey*

PMMA/Ag_2O bone cements with collagen coating were prepared in order to improve their biomineralisation, biocompatibitity and antibacterial properties as well. ATR FTIR spectroscopy analysis demonstrated that collagen electrodeposition on their surface depends on the silver content in samples. In vitro tests, performed in simulated body fluid (SBF) during three weeks of SBF incubation, revealed the dissolution profile of Ag^+ from the acrylic matrix, the results being in concordance with antibacterial tests performed against *Escherichia coli* and *Staphylococcus aureus*. The mineralization process upon incubation was confirmed by the surface morphology analyses (SEM) combined with ATR FTIR, which evidenced the phosphate characteristic bands of hydroxyapatite, depending on the silver oxide content in the samples.

(Received April 11, 2011; Accepted April 19, 2011)

Keywords: Acrylic bone cement, Collagen, Antimicrobial activity, SEM, ATR FTIR

1. Introduction

The development of a novel biomimetic implant based on polymer composites has yet to be justified as a valid and effective design for orthopedic implants. An important parameter that can help predict long-term behavior of the prostheses is the permanent displacement, or migration, of the implant relative to bone. This incidence of migration is one of the predominant causes of failure and is mainly due to micromotion, the lack of fixation stability at the bone-implant interface. It was demonstrated [1] the importance of material flexibility and its effects on stress shielding. Materials with a high flexibility tend to have less bone resorption in the calcar region and the stress level in bone is significantly lower. The mechanical environment of the host bone is altered by the implantation of a foreign material and consequently, bone remodeling occurs in order to adapt the bone structure to this new situation [2].

Orthopedic acrylic cements have to fulfill several medical requirements, such as: low values of maximum cure temperature (to avoid thermal necrosis of the bone tissue, during the setting of the cement), moderate sitting time (so that cement does not cure too fast or too slow), high values of compressive strength (allowing the cured cement mantle to withstand the compressive loads involved by normal daily activities) [3]. A new biomaterials generation was born by combining bioactivity, biocompatibility and antibacterial properties of materials, either by antibiotic [4,5] or silver loading [6,7]. The use of antibiotic-loaded bone cement is a well-accepted adjunct in the treatment of infected joint arthroplasty and is gaining further application as a method of prophylaxis. The influence of antibiotic inclusion on cement mechanical properties, specifically fatigue, determines its resistance to crack formation and the long-term in vivo structural integrity

* Correspondsing author: scavalu@rdslink.ro

of the cement. Several factors influence the choice of antibiotic to add to bone cement. The antibiotic must be able to withstand the exothermic temperature of polymerization, be available as a powder, have a low incidence of allergy, and be able to elute from the cement over an appropriate time period. Several bone cements containing antibiotics such as erythromycin, colystin, gentamicin and tobramycin have been commercially available in Europe for many years. On the other hand, silver based antimicrobials capture much attention not only because of the non toxicity of the active Ag^+ to human cells [8,] but because of their novelty being a long lasting biocide with high temperature stability and low volatility. The antimicrobial efficacy of these composites depends on their ability to release the silver ions from these composites upon interaction with biological fluids. Hence, silver doped materials are use as an alternative (or complementary) to antibiotic loaded cements, silver being capable of killing over 650 forms of bacteria, viruses [9]. In the same times, a complete biological integration into the surrounding tissues is a critical step for clinical success of an implant. It has been previously demonstrated that biomimetic coatings consisting either of collagen type I and hydroxyapatite or mineralized collagen are suitable surfaces to enhance cell attachment and proliferation [10, 11].

Collagen comprises 90% of the extracellular matrix of bone and it occupies a key role in the interaction of osteoblasts and their environment.

We have developed in this work a new strategy for orthopedic/dental implants based on both concepts improvement: bioactivity and antibacterial activity by incorporating different concentration of Ag_2O in PMMA bone cement followed by collagen electrodeposition. The study is focused on scanning electron microscopic analysis before and after immersion in SBF and complementary ATR FTIR spectroscopy which evidenced the phosphate characteristic bands of hydroxyapatite, depending on the silver oxide content in the samples.

2. Experimental

The PMMA/Ag_2O samples were prepared using commercial PMMA based cements (BIOLOS3®) as starting material, by mixing the powder polymethyl methacrylate (copolymer) with Ag_2O particles as antimicrobial agent in concentration of 0.5, 1 and 2% (wt/wt) with respect to the total powder amount and the polymerization was initiated by adding an appropriate volume of liquid monomer (methyl methacrylate). The curing parameters were registered according to the ASTM Standard [12]. Time and temperature were measured from the onset of the mixing powder with the liquid. Two determinations were performed for each sample formulation. The electrodeposition of soluble collagen type I, from calf skin (Sigma Chemicals) was performed for each specimen using a three electrode electrochemistry system, following the protocol described in our previous paper [13]. The first evidence of collagen layer on the surfaces was obtained by recording the ATR FTIR spectra comparing the coated and uncoated surfaces of the samples, using a Spectrum BX II Perkin Elmer spectrometer, equipped with MIRacle ATR accessory (ZnSe crystal), with a scanning speed of 32 cm^{-1} min^{-1} and the spectral width 2.0 cm^{-1}. Deconvolution of amide I band of native collagen and adsorbed on the samples surfaces was performed in order to investigate the conformational changes of the protein during the coating process.

The spectra were smoothed with a 9-point Savitsky–Golay smooth function to remove the white noise. The second derivative spectral analysis of amide I band was applied to locate positions and assign them to different functional groups. Before starting the fitting procedure, the obtained depths of the minima in the second derivative spectrum and subsequently, the calculated maximum intensities, were corrected for the interference of all neighbouring peaks. All second-derivative spectra, calculated with the derivative function of Opus software, were baseline-corrected, based on the method of Dong and Caughey [14] and area-normalized under the second derivative amide I region, 1700–1600 cm^{-1}. Curve fitting was performed by setting the number of component bands found by second-derivative analysis with fixed bandwidth (12 cm^{-1}) and Gaussian profile. The area under each peak was used to calculate the percentage of each component and, finally, to analyze the percentage of secondary structure component [15].

In vitro tests were carried out in Simulated body fluid (SBF), prepared according to Kokubo protocol [16]. Electrochemical measurements were performed in SBF in static conditions,

upon incubation of the materials during three weeks (with and without collagen coating), using a CyberComm 6500 Multimeter (EUTECH Instruments) equipped with Ag^+ ion selective electrodes and data aquisition software. The detection limit using this method is 10^{-6} M for Ag^+ ions. The second evidence of collagen coating was revealed by SEM analysis on the surfaces, as well as the morphology before and after three weeks incubation in SBF. Microstructure characterization was made by using JEOL JSM 7000F Field Emission Scanning Electron Microscope.

Antimicrobial activity of the specimens (cylindrical shape, 10 mm diameter and 3 mm high) was determined against the bacterial pathogens (*Escherichia coli ATCC 2732 and Staphylococcus aureus ATCC 6538 P*) by the agar disc diffusion assay, in Petri dishes (measuring 120 mm each side) containing 20 mL of nutrient agar with 10^5CFU/mL of bacteria. The plates were incubated at 37^0C for 24 h. The antibacterial activity was evaluated by measuring the zone of growth inhibition surrounding the discs.

3. Results and discussions

In spite of its promising bioactivity, the previously reported collagen/calcium phosphate composite [17] is mechanically weak and consequently limited to non-loading applications. An alternative way to improve the mechanical properties of such composites is to apply a collagen layer and such designs are commonly used in medical devices as hip implants. Thus, the bioactive surface would accelerate bone growth and implant fixation, thereby shortening the healing period of the patient. The coating procedure by electrodeposition was already reported [13] using chronoamperometric method. Briefly, a three-electrode electrochemistry system was used by keeping the working electrode at the potential value -2V during 1800 seconds, the current during electrodeposition being monitored by a potentiostat. The current intensity dropped dramatically in the first few minutes of deposition, then remained relatively constant until ~ 20 min. The rapid decrease in intensity represents the capacitive charging of the electrode, followed by a bearing with approximately constant intensity, limited by the diffusion of collagen concentration. Collagen solution was prepared in a concentration of 1 mg/mL of electrolyte and pH was adjusted to 4.8-5.3.

ATR FTIR spectrometric measurement was carried out to further clarify the presence of collagen coating on the surface of each specimen containing different Ag_2O concentration. The spectra recorded before and after collagen electrodeposition on PMMA- based bone cement are presented comparatively for each specimen in fig. 1-3 along with the corresponding spectra recorded after 20 days incubation in Simulated Body Fluid (SBF). The marker bands of PMMA are a sharp and intense peak at 1720 cm^{-1} due to the presence of ester carbonyl group ν(C=O) stretching vibration, a broad band at 1436 cm^{-1} due to $\delta(CH_3)$ vibration mode, the peaks in the range 1265-1000 cm^{-1} assigned to O-C-O, C-CH_3 and C-COO stretching vibrations, and the region between 980-800 cm^{-1} due to the bending of C-H bond [18, 19]. The PMMA characteristic vibrations are very similar for all the three specimens prepared in this study, containing respectively 0.5, 1 and 2% Ag_2O. The ATR FTIR spectra recorded after electrodeposition confirms the presence of the collagen on the specimens surface throughout the characteristics of the distinct peaks of collagen: amide I at 1635/1638 cm^{-1} (C=O stretching), amide II at 1553/1556 cm^{-1} (N-H deformation) and amide III around 1240 cm^{-1} (combined N-H bending and C-N stretching). The relative intensity of these bands is very different with respect to each specimen showing that the collagen deposition depends on the silver concentration in the samples. In the same time, the characteristic bands of PMMA are obviously reduced in intensity as the collagen layer is formed on the surfaces. The results are in accordance with previous reported study regarding collagen self assembly coating by electrolysis on silicate cathode surface [20]. The bioactivity of the surface layer of the specimens was demonstrated by the spectra recorded after 21 days incubation in SBF as shown in Fig. 1c, 2c and 3c. A pronounced decreased in intensity of the bands related to the polymer matrix and to the collagen layer is observed when compare with the corresponding spectra before incubation. Especially for the amide I and II bands of collagen, a broadening and shift to lower wavenumbers was found. The surface mineralization was demonstrated by the strong band at 1015/1020 cm^{-1} which are the characteristics of the calcium phosphate in hydroxyapatite- type biomimetic coatings [10,21, 22]. The appearance of a new band

as a shoulder at 1086/1082 cm^{-1} is also an indicative of the P-O antisymmetric vibration. Thus, as already reported [23], the cations as well as the anions in SBF can be readily and reversibly exchanged.

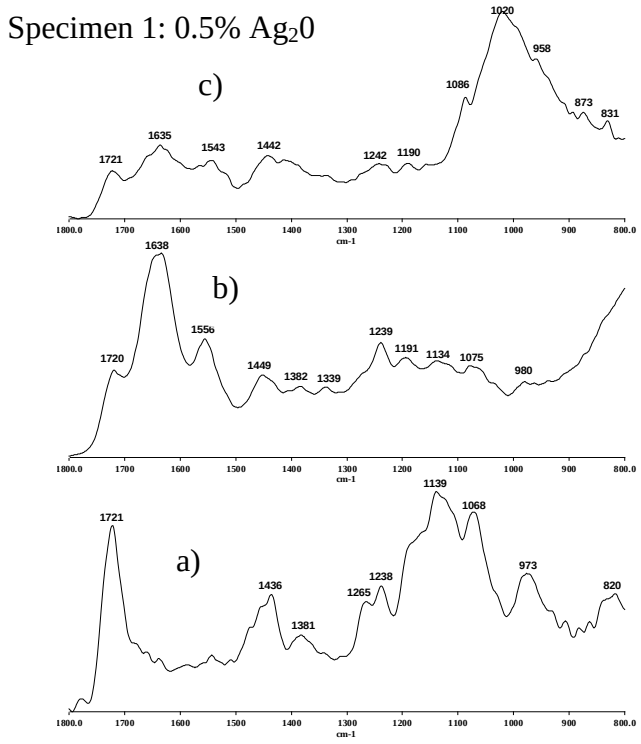

Fig. 1 ATR FTIR spectra of the specimen with 0.5% Ag_20 recorded before (a) and after collagen electrodeposition (b) and upon 20 days incubation in SBF (c).

The hydrated collagen layer is not stable and it is progressively replaced by apatite during ageing in an aqueous media (maturation). The mechanism of this transformation is not yet well known but it involves a decrease of the amount of HPO_4^{2-} ions and an increase of the calcium content of the mineral phase. Simultaneously OH^- ions are included in the structure and water is excluded [24].

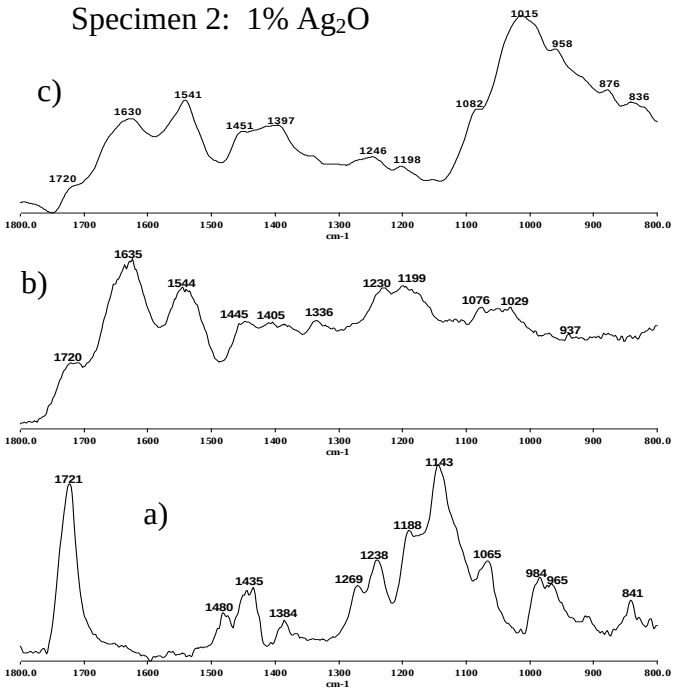

Fig. 2 ATR FTIR spectra of the specimen with 1% Ag_20 recorded before (a) and after collagen electrodeposition (b) and upon 20 days incubation in SBF (c).

The primer condition imposed to materials considered for biomedical applications is biocompatibility dictated by the manner in which their surface interact with blood constituents (erythrocytes, platelets) as well as the proteins [25, 26]. The type and amounts of adsorbed proteins mediate subsequent adhesion, proliferation and differentiation of cells as well as depositing of mineral phases. The behavior of a protein at an interface is likely to differ considerably from its behavior in the bulk.

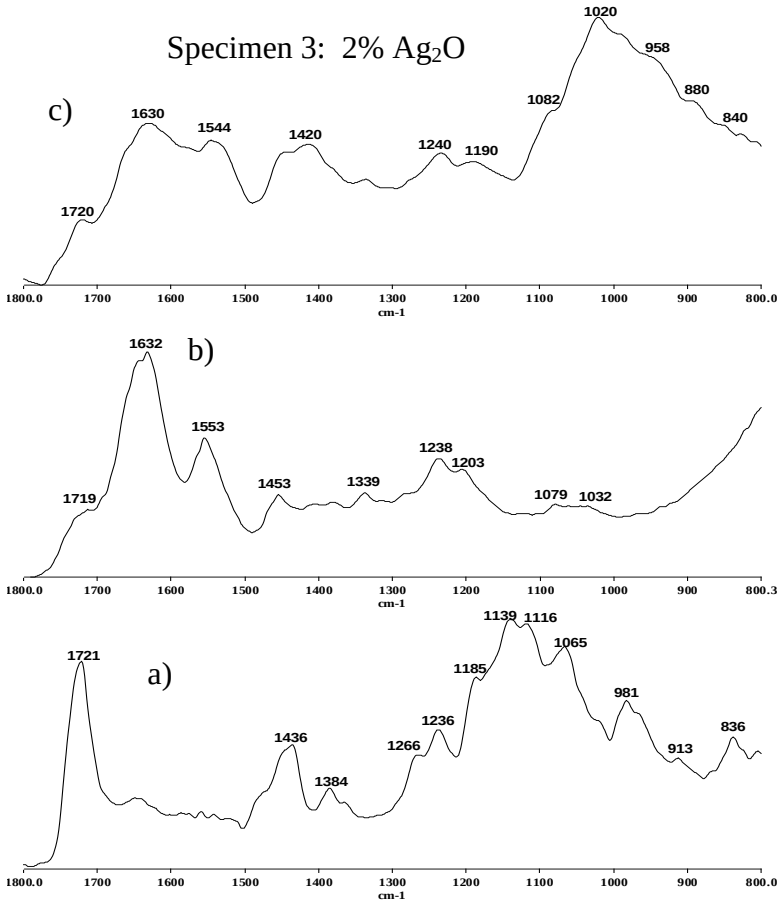

Fig. 3 ATR FTIR spectra of the specimen with 2% Ag_20 recorded before (a) and after collagen electrodeposition (b) and upon 20 days incubation in SBF (c).

Because of the different local environment at the interface, the protein may have the opportunity of adopting a more disordered state exposing its hydrophobic core to the aqueous phase, often called surface denaturation. Denaturation is a process by which hydrogen bonds, hydrophobic interactions and salt linkages are broken and the protein is unfolded. The denaturation of secondary structure involves also changes in ratio among the three common structures: α helix, β sheets or turns and unordered [14, 27]. FTIR spectroscopy can be used to study protein secondary structure in any state, i.e. aqueous, frozen, dried or even as an insoluble aggregate, and for this reason it is one of the most used techniques for studying stress induced alterations in protein conformation and for quantifying protein secondary structure. ATR-FTIR can provide important information leading to the development of novel biomaterials as replacements for damaged or diseased natural tissue. The spectral region of amide I (~1640

cm^{-1}), amide II (~1540 cm^{-1}) and amide III (~1240cm^{-1}) are very sensitive to the conformational changes in the secondary structure of proteins. Computational techniques based on the second derivative spectra and deconvolution procedure is used for percentage evaluation of each secondary structure and also the perturbations upon the adsorption to different surfaces [28,29]. Collagen type I is the most abundant protein of the extracellular matrix, a fibrillar triple helical structure that forms gel networks in irregular connective tissue. Collagen is also proline-rich and self assembles into fibrils [30,31].

As a reference, the FTIR spectrum of native collagen is shown in Fig. 4a , pointing out the features characteristic of amide I, II and III which are the most intense vibrational modes. The present study is focused on the amide I behavior, which is due primarily to the stretching vibrations of the peptide carbonyl group. According to the literature, the intensity of amide I band

of collagen decreases markedly upon denaturation, and after deconvolution, four prominent components are present both in the native or denaturated protein spectrum [15,32]. That the relative intensities of these four peaks vary with the extent of collagen-fold or triple helix content speaks to the point that they are clearly conformationally dependent. Specific components within the fine structure of amide I adsorbed collagen is correlated with different states of hydrogen bonding associated with the local conformations of the alpha chain peptide backbones. This heterogeneity can arise either from intrinsic basicity differences in the strengths of the hydrogen bonds associated with the carbonyls [33]. Deconvolution of amide I band of native collagen and adsorbed to our specimens is shown in Fig. 4 (b,c,e) and the assignment of the components in Table 1 was made on the basis of the previous reported studies, along with the quantitative analysis. Curve fits to the amide I native collagen reveals four Gaussian components at 1630, 1644, 1665 and 1682 cm^{-1} representing helix-related hydrogen-bounded set of carbonyls. According to the literature, the highest frequency carbonyl absorption peak represents the weakest H-bonded system [34]. Beside the characteristic frequencies of α helix conformation, the peak located in the higher region, at 1682 cm^{-1}, represent the formation of an antiparallel β-sheet structure (or turns). Both the intensity and the location of the characteristic peaks are modified upon adsorption. As a general behavior, one can observe a shift toward lower frequencies, a decrease in α helix total content and concomitant increase of turn percentage upon adsorption, as a consequence of denaturation.

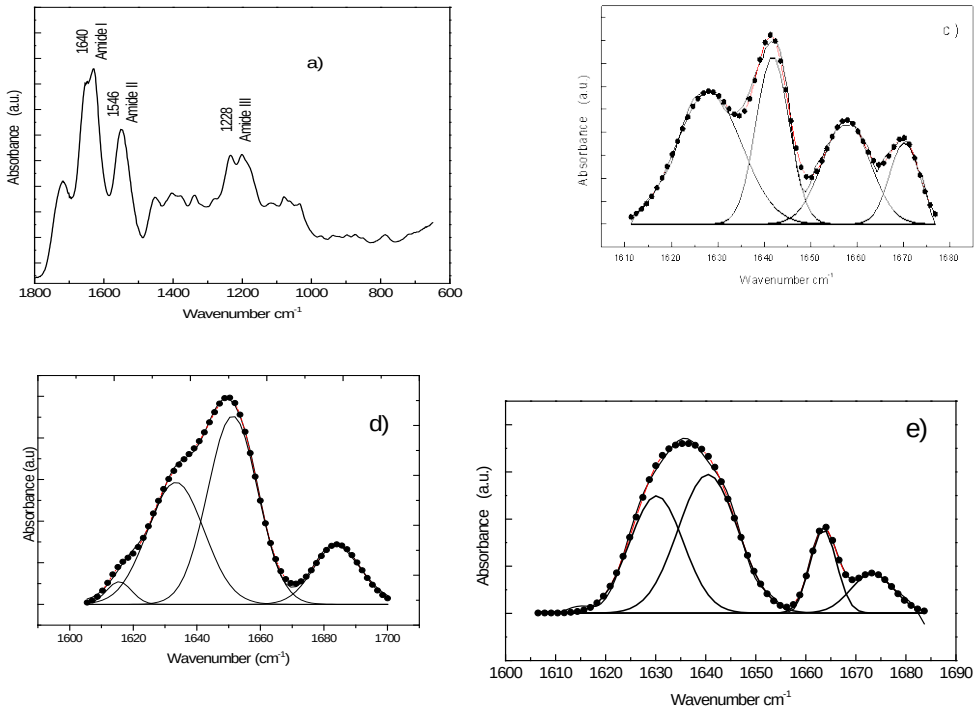

Fig.4. ATR FTIR spectrum of native collagen type I, from calf skin as received from Sigma Chemicals (a), deconvoluted amide I absorption band of native collagen (b) and adsorbed collagen to specimens with 0.5% Ag_20 (c), 1% Ag_20 (d) and 2% Ag_20 (e) respectively.

The silver ion released in simulated body fluid was monitored during 21 days incubation of the three specimens. The results presented in fig. 5 indicate that the silver ion concentration in fluid increase with increasing silver oxide content in the sample. A small amount of silver was detected after the first ten hours of incubation, the Ag^+ release showed only a marginal increase during the first 3 days followed by an abrupt rise after one week especially for composites containing higher silver oxide concentrations. As previousely reported in literature, concentrations of silver ions between 0.10 and 0.22 mM, released from Ag_2O- doped bioactive glass, were found

to have bactericidal activity against gram- positive bacterium [35]. In table 2 are presented the results regarding the antibacterial efficiency of the Ag_2O/PMMA specimens against gram positive (*Staphylococcus aureus ATCC 6538 P)* and gram negative (*Escherichia coli ATCC 2732)*, respective the diameters of the inhibition areas read after 24 hours incubation at 37°C. The inhibition effect is significantly more intense in the case of *Escherichia coli.*

The mechanism of the antimicrobial action of silver ions is not completely known. However, the effect of silver ions on bacteria is linked with its interaction with thiol group compounds found in the respiratory enzymes of the bacterial cells. Silver binds to the bacterial cell wall and cell membrane and inhibits the respiration process. In case of E-coli, silver acts by inhibiting the uptake of phosphate and releasing phosphate, mannitol, succinate, proline and glutamine from the E-coli cells. In addition, it was shown that Ag+ ions prevent DNA replication by binding to the polynucleotide molecules, hence resulting in bacterial death [36].

Table 1.

Collagen amide I	**α helix**		**α helix**		**α helix**		**turns**	
	ν(cm^{-1})	A (%)	ν(cm^{-1})	A (%)	ν(cm^{-1})	A (%)	ν(cm^{-1})	A (%)
native collagen	1630	28.3	1644	33.2	1665	34.7	1682	3.8
Specimen 1 0.5% Ag_2O	1625	40.2	1641	25.5	1657	23.5	1670	10.8
Specimen 2 1% Ag_2O	1619	4.2	1637	37.7	1657	43.5	1682	14.6
Specimen 3 2% Ag_2O	1630	34.0	1640	44.0	1663	12.0	1673	10.0

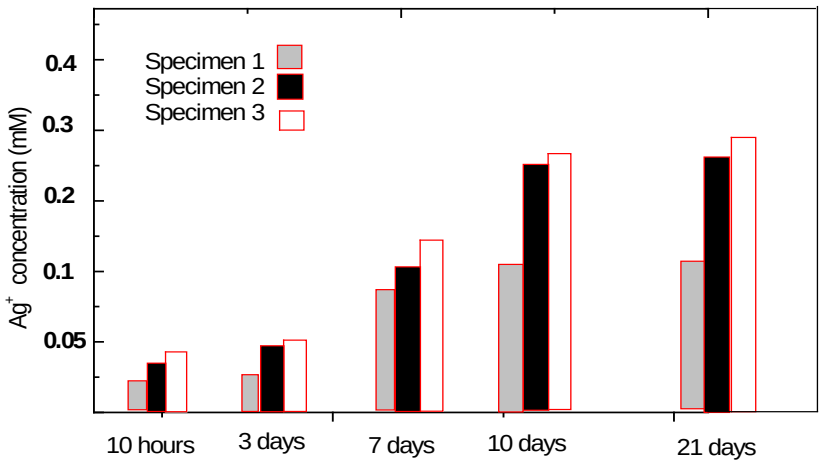

Fig 5. Electrochemical measurements of Ag^+ release from the specimens with different silver oxide content, during 21 days incubation in SBF.

Table 2.

Bacterium	Diameter of inhibition area (mm)/ Specimen		
	0.5% Ag_2O	1% Ag_2O	2% Ag_2O
Staphylococcus aureus ATCC 6538	10.2	12	13.5
Escherichia coli ATCC 2732	12.5	14.2	18

In order to study the morphological details of the samples surfaces, SEM analysis were performed before and after collagen electrodeposition and after 21 days incubation in SBF solution, and presented in fig. 6. Before any treatments (fig. 6 a, b, c) the surfaces presents the granular, regular shape of the PMMA bone cement and dispersed silver oxide particles. After electrodeposition, the images clearly illustrates the formation of collagen films on the sample surfaces (fig.6 d, e, f), covering uniformly the PMMA granules. According to the literature [15], once the protein has covered the surface of implants, host cells are no longer able to contact the underlying foreign-body material but only the protein–coated surface. The adsorbed protein layer- rather then the foreign material itself may stimulate or inhibit further biochemical processes. The bioactivity of the samples was demonstrated by the intense nucleation process of calcium containing crystals (fig. 6 g,h,i), the distribution of the aggregates being densely on the specimen 3 surface. The formation of hydroxyapatite crystals in this case was strongly influenced by the presence of collagen layer, as demonstrated by comparing with our previousely reported study on the bioactivity of silver/PMMA acrylic cements without collagen film [22,23].

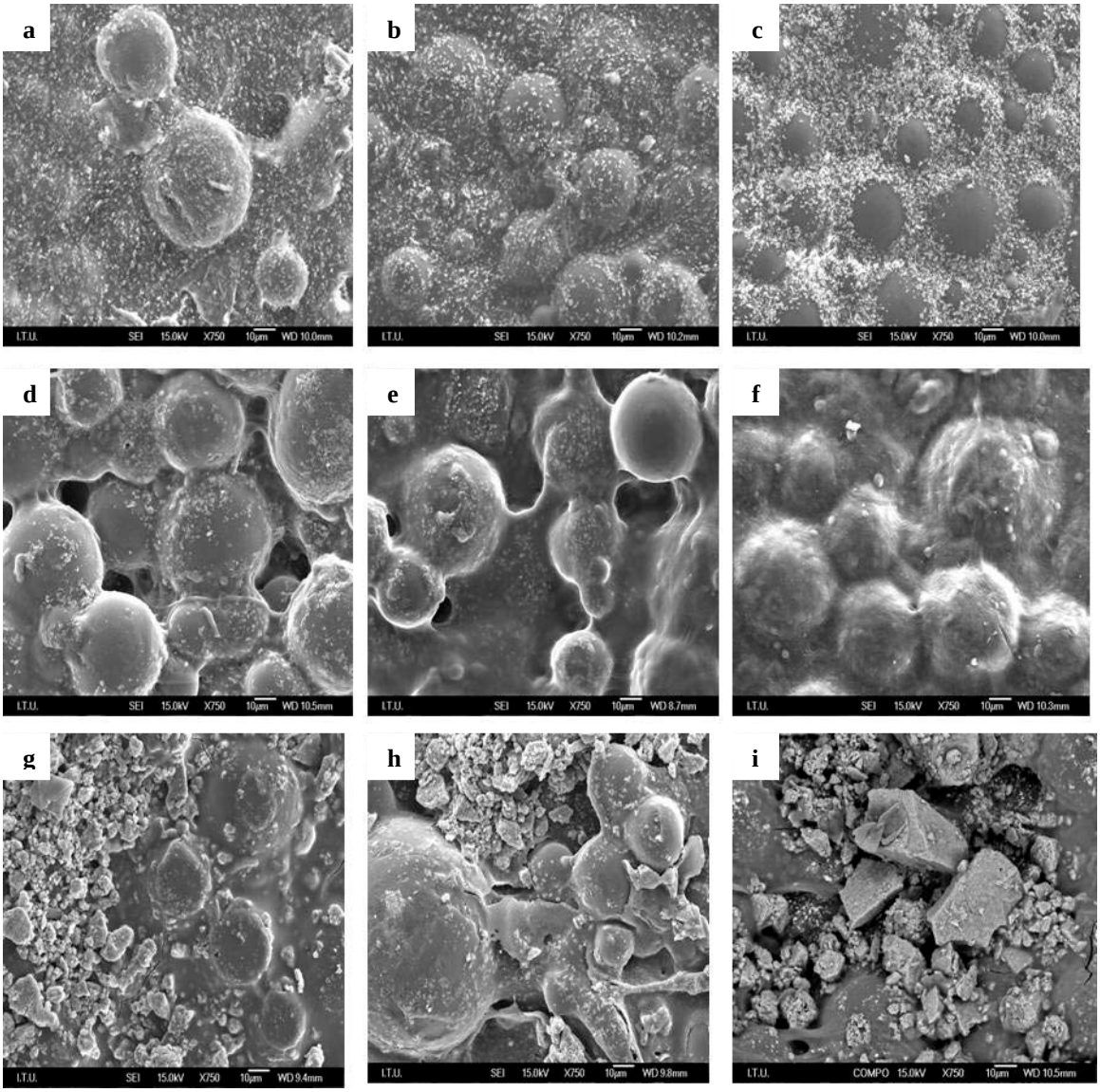

Fig. 6. Surface morphology of the specimens surface, untreated (a, b, c), after collagen electrodeposition (d, e, f) and upon incubation in SBF during 21 days (g, h, i). The images, from left to right correspond to the specimen 1 (0.5%Ag_2O), specimen 2 (1%Ag_2O) and specimen 3 (2%Ag_2O) respecyively.

4. Conclusions

PMMA/ Ag_2O bone cements were prepared by incorporating different silver oxide content as a potential antimicrobial agent and collagen electrodeposition on the surface was realised in order to improve the biomineralisation and biocompatibitity of the materials. The first evidence of collagen layer on the surfaces was obtained by recording the ATR FTIR spectra comparing the coated and uncoated surfaces of the samples. The results showed that collagen adsorption depends on the silver content in samples. Deconvolution spectra of amide I absorbtion band of collegen indicates modifications in secondary structure of collagen structure upon adsorption to specimens containing different concentrations of Ag_2O. In vitro tests, carried out in simulated body fluid, revealed that the materials are capable to release Ag^+ during three weeks incubation indicating that the Ag^+ ion concentration in fluid increases with increasing Ag_2O content in the sample. The antibacterial efficiency of the Ag_2O/PMMA specimens against gram positive (*Staphylococcus*

aureus ATCC 6538 P) and gram negative (*Escherichia coli ATCC 2732)*, bacterium shows that he inhibition effect is significantly more intense in the case of *Escherichia coli.*

The mineralization process upon 21days incubation time was also dependent on the Ag_2O content in the samples. Moreover, the SEM micrographs show that formation of hydroxyapatite crystals was strongly influenced by the presence of collagen layer, but dependent on the silver oxide as well.

Acknowledgements:

This research was accomplished in the framework of Romania-Turkey Bilateral Cooperation, project nr. 385/2010.

References

[1] R. Huiskes, H. Weinans, B. VanRietbergen, Clin Orthop Res **274**, 124 (1997).
[2] F.K. Chang, J. L. Perez, J. A. Davidson, Journal of Biomedical Materials Research, **24**(7), 873 (1990).
[3] M. C. Rusu, D. L. Rusu, M. Rusu, JOAM –Symposia **1**(6,) 1020 – 1026(2009)
[4] Y.He, J.P. Trotignon, B.Loty, A. Tcharkhtchi, J. Verdu, J Biomed Mater Res **63**, 800(2002).
[5] H.Van de Belt, D.Neut, W. Schenk, J.R.Van Horn, H.C. Van der Mei, H. J. Busscher, Acta Orthop Scand **72**, 557(2001).
[6] R.Kumar, H.Munstedt, Biomaterials **26**(14), 2081(2004).
[7] M.Kawashita, S.Tsuneyama, F.Miyaji,T.Kokubo, K.Yamamoto, Biomaterials **21**, 393 (2000).
[8] J.Hardes, A. Streitburger, H. Ahrens, T. Nusselt, C. Gebert, W. Winkelmann, A.Battmann, G. Gosheger, Sarcoma, doi:10.1155/2007/26539 (2007)
[9] A. Gupta, S. Silver, Nat Biotechnol **16**, 888(1998)
[10] Y. Fan, K. Duan, R. Wang, Biomaterials **26**(14) 1623-1632(2005)
[11] S. Roessler, R. Born, D. Scharnweber, H. Worch, J Mater Sci Mater Med **12,** 871-877(2001)
[12] *** American Society for Testing and Materials (ASTM), Standard F451-99a, 2000 Annual Book of ASTM Standard, Vol. 13.01, 55 (2000).
[13] S. Cavalu S., F. Banica , V. Simon , JOAM Symposia, **2**, (1),140 (2010).
[14] A. Dong, W.S. Caughey, Methods Enzymol. **232**, 139 (1994).
[15] S. Tunc, M.F. Maintz, G. Steiner, L. Vasquez, M.T. Pham, R. Salzer, Colloids Surf.B, **42**, 219-225 (2005).
[16]] T. Kokubo, S. Ito, Z.T.Huang, T.Hayashi, S.Sakka, T.Kitsugi, T.Yamamuro, J Biomed Mater Res **24**, 331(1990).
[17] C. Du, F.Z. Cui, W. Zhang, Q.L. Feng, X.D. Zhu, K. De Groot, J. Biomed. Mater. Res. **50**, 518-527(2000).
[18] A. Balamurugan, S. Kannan, V. Selvaraj, S. Rajeswari, Trends Biomater Artif Organs **18**(1) 41(2004).
[19] I. Notinger, J.J. Blaker, V. Maquet, L.L. Hench, A. Boccaccini, Asian J. Physics **15**(2) 221(2006).
[20] J.C. Brodie, J. Merry, M.H. Grant, J. Mater. Sci: Mater Med **17**,43-48 (2006).
[21] S. Roessler, R. Born, D. Scharnweber, H. Worch, J Mater Sci Mater Med **12,** 871-877(2001)
[22] S. Cavalu, V. Simon, J. Optoelectron Adv. Mater. **8**(4) 1520-1523(2006)
[23] S.Cavalu, V.Simon, C. Albon, C. Hozan, JOAM **9**(3) 693-697 (2007**)**
[24] P. Sutandar, D.J.Ahn, E.I.Franses, Macromolecules **27**,7316-7328 (1994)
[25] W. Aken, Steen Dawis ed., Kluwer academic publishers, Norwell, Massachusetts, USA, (1989).
[26] K. Vijayanand, D. K. Pattanayak, T. R. Rama Mohan, R. Banerjee, Trends Biomater. Artif. Organs,**18** (2), 73-83 (2005).
[27] A. Dong, J. D. Meyer, J.L Brown, M.C. Manning, J.F. Carpenter, Arch. Biochem. Biophys. **383**, 148-155 (2000).

[28] G. Damian, S. Cavalu, Asian Chem. Letters, **9**(1-2), 3-9 (2005).
[29] S. Cavalu, V. Simon, JOAM **9**(11), 3297-3302 (2007).
[30] L.J. Juszczak, J. Biol. Chem. **279**(9), 7395-7404 (2004).
[31] S. Leikin, V.A.Parsegian, W.H.Yang, G.E.Walrafen, Proc. Nat. Acad.Sci. USA, **94**, 11312-11317 (1997).
[32] K.J. Payne, A. Veis, Biopolymers, **27**, 1749-1760 (1988).
[33] J. D. Whittle, N.A. Bullett, R.D. Short, C.W. I. Douglas, A.P. Hollander, J. Davies, J. Mater. Chem., **2**, 2726-2732 (2002).
[34] K.J. Payne, A. Veis, Biopolymers, **27**, 1749-1760 (1988).
[35] M. Bellantone, H. D. Williams, L.L. Hench, Antimicrobial Agents and Chemotherapy **46**(6), 1940-1945 (2002).
[36] F. Heidarpour, W. A. Wan AB. Karim Ghani, F. R. Bin Ahmadun, S. Sobri, M. Zargar, M. R. Mozafari, Digest J Nanomat. Biostruct. **5**(3), 797 (2010).